Study of P and CP symmetries in $\Xi_c^+ \to \Xi^-\pi^+\pi^+$ at electron-positron collider

Yunlu Wang (王云路)[1†] Yunlong Xiao (肖云龙)[1‡] Pengcheng Hong (洪鹏程)[2§] Ronggang Ping (平荣刚)[3¶]

[1]Key Laboratory of Nuclear Physics and Ion-beam Application (MOE) and Institute of Modern Physics, Fudan University, Shanghai, China 200433
[2]College of Physics, Jilin University, Changchun, China 130012 and Institute of High Energy Physics, Beijing 100049
[3]Institute of High Energy Physics, Beijing 100049, People's Republic of China and University of Chinese Academy of Science, Beijing 100049, China

Abstract: Symmetry studies represent one of the most promising frontiers in particle physics research. This investigation focuses on exploring P and CP symmetries in the charm system through the measurement of asymmetry decay parameters in the three-body decay of Ξ_c^+. Incorporating electron and positron beam polarization effects and utilizing the helicity formalism, we characterize the decay of Ξ_c^+ and its secondary hyperons through asymmetry decay parameters. The complete angular distribution formula for these decays has been systematically derived. Our study evaluates the sensitivity of the asymmetry parameters for the $\Xi_c^+ \to \Xi^-\pi^+\pi^+$ decay channel under various data sample sizes and beam polarization scenarios. These findings establish a robust theoretical framework for future experimental studies at the STCF, providing valuable insights for symmetry investigations in the charm sector.

Keywords: Symmetry, polarization, baryon

DOI: **CSTR:**

I. INTRODUCTION

Charge parity (CP) violation is one of the three fundamental conditions required to explain the matter-antimatter asymmetry observed in the universe [1]. In the Standard Model of particle physics, the quark dynamics are descried by the Cabibbo-Kobayashi-Maskawa (CKM) mechanism [2, 3]. While the CP violation observed in the decays of K, B, and D mesons is well described by the CKM mechanism [4−10], it remains insufficient to account for the observed matter-antimatter asymmetry in the universe [11]. Given that the observable universe is predominantly composed of baryons, studying CP violation in baryon decays is crucial for understanding this asymmetry. Recent experimental advancements have provided compelling evidence for CP violation in Λ_b baryons. For instance, the evidence of CP violation in $\Lambda_b \to \Lambda K^+K^-$ [12] decay and the first observation of CP violation in the four-body decay of $\Lambda_b \to pK^-\pi^+\pi^-$ [13] have been reported at the LHCb experiment. However, current research on CP violation primarily focuses on Λ_b decays, making it challenging to directly compare theoretical predictions involving baryon decays without b-quarks. This highlights the need to explore CP violation in other baryonic systems. The two-body decay processes of baryons can be parameterized using decay parameters α and $\bar{\alpha}$. Parity violation in baryons and anti-baryons is indicated by non-zero values of α and $\bar{\alpha}$ [14]. Experimentally, CP symmetry is tested by comparing the decay parameters of baryons and anti-baryons through the CP-odd observable $\mathcal{A}_{CP} = (\alpha+\bar{\alpha})/(\alpha-\bar{\alpha})$ [15−19]. Here, α and $\bar{\alpha}$ represent the decay parameters of the baryon and anti-baryon, respectively. A non-zero measurements of α and $\mathcal{A}_{CP}$ signify parity (P) and CP violations [20−24]. While two-body decays of baryons have been extensively studied, identifying new sources of CP violation in baryon decays without b-quarks is essential to unravel this mystery and represents a critical frontier in CP violation research.

The Cabibbo-favored three-body decay of the charmed baryon, $\Xi_c^+ \to \Xi^-\pi^+\pi^+$, involves both external and internal W-emission modes, with decay amplitudes comprising factorizable and non-factorizable contributions. The total branching fractions of $\Xi_c^+ \to \Xi^-\pi^+\pi^+$ and its isospin channel $\Xi_c^+ \to \Xi^0\pi^0\pi^+$ are approximately 10%, making them the most probable decay modes [25]. Con-

Received 15 July 2025; Accepted 21 October 2025

† E-mail: yunluwang20@fudan.edu.cn
‡ E-mail: xiaoyunlong@fudan.edu.cn(Corresponding author)
§ E-mail: hongpc@ihep.ac.cn
¶ E-mail: pingrg@ihep.ac.cn

sequently, these channels are expected to yield abundant experimental data, facilitating the investigation of P and CP violations at future facilities such as the Super Tau-Charm Facility (STCF) [26].

The parameters for three-body decays cannot be directly described by the Lee-Yang formalism [27]. Therefore, it is necessary to define analogous decay parameters through decay amplitudes to study P and CP violations. In electron-positron collisions, the threshold energy for the process $e^+e^- \to \Xi_c^+\bar{\Xi}_c^-$ is above 4.94 GeV. Both the upgraded BESIII experiment and the future STCF are expected to produce Ξ_c^+ and $\bar{\Xi}_c^-$ pairs. Precision measurements of the decay parameters for $\Xi_c^+ \to \Xi^-\pi^+\pi^+$ and its isospin process $\Xi_c^+ \to \Xi^0\pi^0\pi^+$ will provide critical insights to validate or exclude existing theoretical models and test isospin symmetry through comparative decay parameters.

The amplitude for decay $\Xi_c^+(\lambda_1) \to \Xi^-(\lambda_2)\pi^+\pi^+$ would indicate all information about spin and helicity of the particles. In helicity formalism, the amplitude is model-independent and expressed by $B_\mu^J(\lambda_2,0,0)$ which has the sum of resonances in Eq. (2). Here $J=\frac{1}{2}$ is the spin of mother particle, μ is its eigenvalue in the body-fixed z-axis that can be $\frac{1}{2}$ or $-\frac{1}{2}$, and $\lambda_2 = \pm\frac{1}{2}$ is the helicity of Ξ^-. Then there are four degrees of freedom $B^{\frac{1}{2}}_{\frac{1}{2}}(\frac{1}{2},0,0)$, $B^{\frac{1}{2}}_{-\frac{1}{2}}(\frac{1}{2},0,0), B^{\frac{1}{2}}_{\frac{1}{2}}(-\frac{1}{2},0,0)$, and $B^{\frac{1}{2}}_{-\frac{1}{2}}(-\frac{1}{2},0,0)$, which are denoted by $B^\mu_{\lambda_2}$ for simplification.

Similarly, the production of Ξ_c^+ and decay of Ξ^- are also written in helicity formalism, and the corresponding amplitudes are listed in Table 1. If the parity is conserved [28], the four amplitudes should satisfy the relations $B^+_{\frac{1}{2}} = -B^+_{-\frac{1}{2}}$ and $B^-_{\frac{1}{2}} = B^-_{-\frac{1}{2}}$. However, the weak decay process $\Xi_c^+ \to \Xi^-\pi^+\pi^+$ allows for parity violation. To characterize parity violation in this process, three asymmetry parameters can be defined by following formula:

$$\begin{aligned}
\alpha_{\Xi_c^+} &= \frac{|B^+_{\frac{1}{2}}|^2 - |B^+_{-\frac{1}{2}}|^2}{|B^+_{\frac{1}{2}}|^2 + |B^+_{-\frac{1}{2}}|^2},\\
\beta_{\Xi_c^+} &= \frac{|B^-_{\frac{1}{2}}|^2 - |B^-_{-\frac{1}{2}}|^2}{|B^-_{\frac{1}{2}}|^2 + |B^-_{-\frac{1}{2}}|^2},\\
\gamma_{\Xi_c^+} &= \frac{|B^+_{\frac{1}{2}}|^2 + |B^+_{-\frac{1}{2}}|^2}{|B^-_{\frac{1}{2}}|^2 + |B^-_{-\frac{1}{2}}|^2}.
\end{aligned} \tag{1}$$

They are an extended definitions from two-body decay, based on asymmetry parameters in terms of partial wave amplitudes from Lee-Yang [27] but in helicity formalism. The parameter $\gamma_{\Xi_c^+}$ represents the relative magnitude of the two types of degenerate amplitudes.

The decay $\Xi_c^+ \to \Xi^-\pi^+\pi^+$ may include intermediate resonance processes from three two-body decays: $\Xi_c^+ \to \Xi(1530)^0\pi^+ \to \Xi^-\pi^+\pi^+$, $\Xi_c^+ \to \Xi(1620)^0\pi^+ \to \Xi^-\pi^+\pi^+$, and $\Xi_c^+ \to \Xi(1690)^0\pi^+ \to \Xi^-\pi^+\pi^+$. Among these, the first process is suppressed due to the spin of $\Xi(1530)^0$ being $\frac{3}{2}$. The intermediate states $\Xi(1620)^0$ and $\Xi(1690)^0$ are allowed and can also be described by our method. The amplitudes are model-independent and are relative to intermediate states by the integration:

Table 1. Helicity angles and amplitudes in relative decays.

decay	helicity angle	helicity amplitude
$\gamma^* \to \Xi_c^+(\lambda_1)\bar{\Xi}_c^-(\lambda_0)$	(θ_1,ϕ_1)	A_{λ_1,λ_0}
$\Xi_c^+(\lambda_1) \to \Xi^-(\lambda_2)\pi^+\pi^+$	(ϕ_2,θ_2,ψ_2)	$B^\mu_{\lambda_2}$
$\Xi^-(\lambda_2) \to \Lambda(\lambda_3)\pi^-$	(θ_3,ϕ_3)	F_{λ_3}
$\Lambda(\lambda_3) \to p(\lambda_4)\pi^-$	(θ_4,ϕ_4)	H_{λ_4}

$$|B^\mu_{\lambda_2}|^2 = \int d\Phi_3 |\tilde{B}^\mu_{\lambda_2}(m_{\Xi^-\pi^+}, m_{\Xi^-\pi'^+}, m_{\pi^+\pi'^+})|^2, \tag{2}$$

where $m_{\Xi^-\pi^+}$ and $m_{\Xi^-\pi'^+}$ are the invariant mass of Ξ^- with two pions respectively, also are treated as Dalitz plots variables [29] and the space $d\Phi_3$ consists of Euler angles given in Table 1. The $m_{\pi^+\pi'^+}$ is invariant mass of two pions. The integration can be estimated by using Monte-Carlo method but is out of this study, so we keep the amplitudes arbitrary for generality, and clarify the magnitude and phase angle of an amplitude by denoting $B^+_{\lambda_2} = b^+_{\lambda_2} e^{i\zeta^+_{\lambda_2}}$, then the four magnitudes can be rewritten in terms of the asymmetry parameters as

$$\begin{aligned}
(b^+_{\frac{1}{2}})^2 &= 1,\\
(b^+_{-\frac{1}{2}})^2 &= \frac{1-\alpha_{\Xi_c^+}}{1+\alpha_{\Xi_c^+}},\\
(b^-_{\frac{1}{2}})^2 &= \frac{1+\beta_{\Xi_c^+}}{\gamma_{\Xi_c^+}(1+\alpha_{\Xi_c^+})},\\
(b^-_{-\frac{1}{2}})^2 &= \frac{1-\beta_{\Xi_c^+}}{\gamma_{\Xi_c^+}(1+\alpha_{\Xi_c^+})}.
\end{aligned} \tag{3}$$

Analogous to Eq. (1), the asymmetry parameters $\alpha_{\bar{\Xi}_c^-}$, $\beta_{\bar{\Xi}_c^-}$, and $\gamma_{\bar{\Xi}_c^-}$ for decay of the antibaryon $\bar{\Xi}_c^- \to \bar{\Xi}^+\pi^-\pi^-$ have similar expressions. With those parity parameters, the CP violation can be characterized by

$$\begin{aligned}
\mathcal{A}_{CP} &= \frac{\alpha_{\Xi_c^+} + \alpha_{\bar{\Xi}_c^-}}{\alpha_{\Xi_c^+} - \alpha_{\bar{\Xi}_c^-}},\\
\mathcal{B}_{CP} &= \frac{\beta_{\Xi_c^+} + \beta_{\bar{\Xi}_c^-}}{\beta_{\Xi_c^+} - \beta_{\bar{\Xi}_c^-}},\\
C_{CP} &= \frac{\gamma_{\Xi_c^+} - \gamma_{\bar{\Xi}_c^-}}{\gamma_{\Xi_c^+} + \gamma_{\bar{\Xi}_c^-}},
\end{aligned} \tag{4}$$

which have an advantage that the systematic uncertainties of production and detection asymmetries are largely

cancelled [30]. The parameters can be written in other expressions after inserting partial amplitudes. For example, the leading-power expansion of the first parameter is reduced to [15, 31]

$$\mathcal{A}_{CP} \propto -\tan\Delta\delta\tan\Delta\phi, \tag{5}$$

where the relative strong phase $\Delta\delta$ depends on final states, and the weak phase $\Delta\phi$ stems from interference between amplitudes with different partial wave configurations in the same decay [32]. The amplitudes partially derive from tree and penguin diagrams like the examples shown in Fig. 1, where the interfered CKM matrix elements $V_{cs}^* V_{ud} \times V_{cb}^* V_{tb} V_{ts}^* V_{ud}$ and their conjugations give rise to the nonzero phase $\Delta\phi$.

The tree diagram is Cabibbo-favored, while the penguin diagram is suppressed from off-diagonal elements $V_{cb}^* V_{ts}^*$. Following the measured values of CKM matrix [25], the magnitude of the weak phase shift is about $\mathrm{Im}[-(V_{cb}^* V_{tb} V_{ts}^* V_{ud})]$ and expected at order of $O(10^{-4}\sim 10^{-5})$. Due to the possible suppression of the strong phase, the magnitude of CP violation is expected to be smaller than the expected value, and the interference effect between the two figures in Fig. 1 also tends to suppress the observation of the violation. If an enhancement of CP violation is observed, it arises from a combination of direct CP violation and potential new physics contributions. To determine these effects, further measurements need to be performed at STCF in the future.

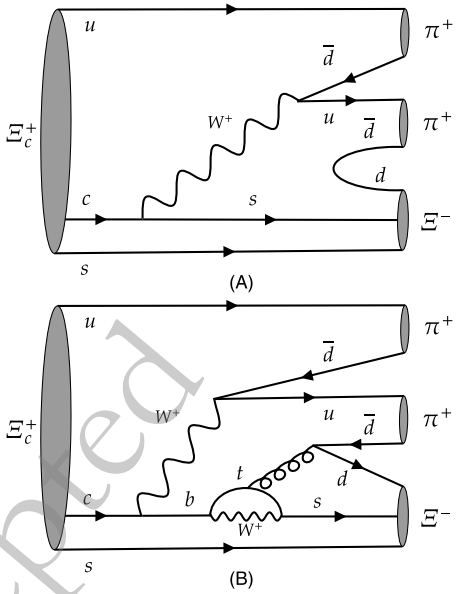

Fig. 1. Tree and penguin diagrams as examples for $\Xi_c^+ \to \Xi^-\pi^+\pi^+$ decay.

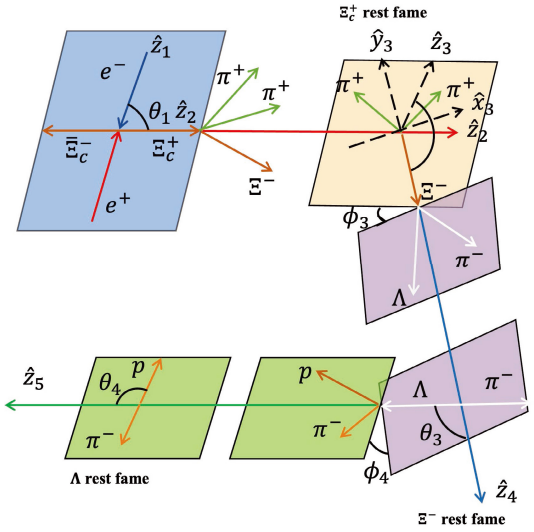

Fig. 2. (color online) Definition of helicity frame at e^+e^- collider.

II. HELICITY SYSTEM

In this analysis, we adopt a helicity frame to describe the decay chain [28]. The helicity angles and amplitudes of the $\Xi_c^+\bar{\Xi}_c^-$ production and decay are listed in Table 1, and the corresponding angles are also shown in Fig. 2. The momentum p_i are obtained by boosting particle i to the rest frame of its mother particle.

The angle between the Ξ_c^+ production and the collision plane is defined as ϕ_1. For the three-body decay of $\Xi_c^+ \to \Xi^-\pi^+\pi^+$, the Euler angles (ϕ_2,θ_2,ψ_2) are used. The system is rotated from $\hat{z}_2$ to $\hat{z}_3$ following the ZYZ convention. In Ξ^- decays, a rotation from $\hat{z}_3$ to $\hat{z}_4$ is needed. Due to the rotational invariance of helicity, this rotation operation does not introduce any additional modifications. In fact, the angle ψ_2 will not contribute to integrated cross sections we are interested in, and the selection of pion does not alter amplitudes since the meson's spin is zero.

III. ANGULAR DISTRIBUTIONS

The spin and polarization information of particles can be encoded in spin density matrix (SDM) [33, 34]. The SDM of spin-$\frac{1}{2}$ particles like Ξ_c^+ is expressed by a 2×2 matrix:

$$\rho^{\Xi_c^+} = \frac{\mathcal{P}_0}{2}\begin{pmatrix} 1+\mathcal{P}_z & \mathcal{P}_x - i\mathcal{P}_y \\ \mathcal{P}_x + i\mathcal{P}_y & 1-\mathcal{P}_z \end{pmatrix},$$

where $\mathcal{P}_0$ carry the unpolarized information. Polarization $\mathcal{P}_z$ is longitudinal part, while the information of transverse polarization is taken by $\mathcal{P}_x$ and $\mathcal{P}_y$. To obtain their explicit expressions, transfer functions starting from initial collision will be solved in the following sections.

A. Ξ_c^+ production on e^+e^- collider

The SDM of Ξ_c^+ from polarized virtual photon can be written as

$$\rho^{\Xi_c^+}_{\lambda_1,\lambda_1'} \propto \sum_{\lambda,\lambda_0} \rho^{\gamma^*}_{\lambda,\lambda'} D^{1*}_{\lambda,\lambda_1-\lambda_0}(\phi_1,\theta_1,0) \times D^{1}_{\lambda',\lambda_1'-\lambda_0}(\phi_1,\theta_1,0) A_{\lambda_1,\lambda_0} A^*_{\lambda_1',\lambda_0}, \tag{6}$$

where $D^J_{\lambda_j,\lambda_k}$ is the Wigner-D function. For polarized symmetric e^+e^- beams, if the transverse polarization information is considered, the SDM of photon is given by [35]

$$\rho^{\gamma^*}_{\lambda_0,\lambda_0'} = \frac{1}{2}\begin{pmatrix} 1 & 0 & p_T^2 \\ 0 & 0 & 0 \\ p_T^2 & 0 & 1 \end{pmatrix}, \tag{7}$$

where the range of transverse polarization p_T satisfies $0 < p_T < 1$. Carrying out Eq. (6) under parity conversation, we get the unpolarized cross section which depends on the polarization of virtual photon, that is

$$\mathcal{P}_0 = 1 + \alpha_c \cos^2\theta_1 + p_T^2 \alpha_c \sin^2\theta_1 \cos 2\phi_1 . \tag{8}$$

The constant $\frac{1}{2}|A_{\frac{1}{2},-\frac{1}{2}}|^2 + |A_{\frac{1}{2},\frac{1}{2}}|^2$ is suppressed, since it does not contribute to the final normalized cross sections. The angular distribution parameter α_c for $e^+e^- \to \Xi_c^+\bar{\Xi}_c^-$ is defined by

$$\alpha_c = \frac{|A_{\frac{1}{2},-\frac{1}{2}}|^2 - 2|A_{\frac{1}{2},\frac{1}{2}}|^2}{|A_{\frac{1}{2},-\frac{1}{2}}|^2 + 2|A_{\frac{1}{2},\frac{1}{2}}|^2}. \tag{9}$$

The transverse and longitudinal polarizations of Ξ_c^+ are

$$\begin{aligned} \mathcal{P}_x &= \frac{-p_T^2\sqrt{1-\alpha_c^2}\sin\Delta_1\sin\theta_1\sin 2\phi_1}{1+\alpha_c\cos^2\theta_1 + p_T^2\alpha_c\sin^2\theta_1\cos 2\phi_1}, \\ \mathcal{P}_y &= \frac{\sqrt{1-\alpha_c^2}\sin\Delta_1\sin\theta_1\cos\theta_1(1-p_T^2\cos 2\phi_1)}{1+\alpha_c\cos^2\theta_1 + p_T^2\alpha_c\sin^2\theta_1\cos 2\phi_1}, \\ \mathcal{P}_z &= 0, \end{aligned} \tag{10}$$

where Δ_1 represents phase angle difference $\Delta_1 = \zeta_{\frac{1}{2},-\frac{1}{2}} - \zeta_{\frac{1}{2},\frac{1}{2}}$. In symmetric electron-positron collision experiments, the transverse polarization of the positron and electron beams directly influences the transverse polarization of Ξ_c^+ as well as $\bar{\Xi}_c^-$. Though the measured values of the parity parameter of this process is lack, in the following sections we use $\alpha_c = 0.7$ and $\Delta_1 = \pi/6$ which are close to the measurements of strange baryons [36].

B. $\Xi_c^+(\lambda_1) \to \Xi^-(\lambda_2)\pi^+\pi^+$

The information of parity violation of this three-body decay is carried by the SDM of Ξ^-, which is given by transfer equation:

$$\rho^{\Xi^-}_{\lambda_2,\lambda_2'} \propto \sum_{\lambda_1,\lambda_1',\mu} \rho^{\Xi_c^+}_{\lambda_1,\lambda_1'} D^{\frac{1}{2}*}_{\lambda_1,\mu}(\phi_2,\theta_2,\psi_2) \times D^{\frac{1}{2}}_{\lambda_1',\mu}(\phi_2,\theta_2,\psi_2) B^{\mu}_{\lambda_2} B^{\mu*}_{\lambda_2'}, \tag{11}$$

where μ is the z-component of angular momentum of Ξ_c^+ whose quantization axis itself rotates under the rotation of the system. After summing all combinations and implementing simplifications, the polarization operators of Ξ^- reduce to

$$\begin{aligned} \mathcal{P}_0^{\Xi^-} &= \frac{\mathcal{P}_0}{2}\left(f_+^{\Xi^-} + f_-^{\Xi^-}\mathcal{P}_{xy}\sin\theta_2\right), \\ \mathcal{P}_0^{\Xi^-}\mathcal{P}_z^{\Xi^-} &= \frac{\mathcal{P}_0}{2}\left(g_+^{\Xi^-} + g_-^{\Xi^-}\mathcal{P}_{xy}\sin\theta_2\right), \\ \mathcal{P}_0^{\Xi^-}\mathcal{P}_x^{\Xi^-} &= \mathcal{P}_0\Big[\cos\Delta^+\left(1+\mathcal{P}_{xy}\sin\theta_2\right) b^+_{\frac{1}{2}} b^+_{-\frac{1}{2}} \\ &\quad + \cos\Delta^-\left(1-\mathcal{P}_{xy}\sin\theta_2\right) b^-_{\frac{1}{2}} b^-_{-\frac{1}{2}}\Big], \\ \mathcal{P}_0^{\Xi^-}\mathcal{P}_y^{\Xi^-} &= -\mathcal{P}_0\Big[\sin\Delta^+\left(1+\mathcal{P}_{xy}\sin\theta_2\right) b^+_{\frac{1}{2}} b^+_{-\frac{1}{2}} \\ &\quad + \sin\Delta^-\left(1-\mathcal{P}_{xy}\sin\theta_2\right) b^-_{\frac{1}{2}} b^-_{-\frac{1}{2}}\Big], \end{aligned} \tag{12}$$

where the functions $f_\pm^{\Xi^-}$ and $g_\pm^{\Xi^-}$ carry the dynamical information of the decay via Eq. (3) and are defined by

$$\begin{aligned} f_\pm^{\Xi^-} &= (b^+_{\frac{1}{2}})^2 + (b^+_{-\frac{1}{2}})^2 \pm \left[(b^-_{\frac{1}{2}})^2 + (b^-_{-\frac{1}{2}})^2\right], \\ g_\pm^{\Xi^-} &= (b^+_{\frac{1}{2}})^2 - (b^+_{-\frac{1}{2}})^2 \pm \left[(b^-_{\frac{1}{2}})^2 - (b^-_{-\frac{1}{2}})^2\right]. \end{aligned} \tag{13}$$

Especially, there are $g_\pm^{\Xi^-} = 0$ when parity is conserved. The transverse information from Ξ_c^+ is involved via the definition $\mathcal{P}_{xy} = \mathcal{P}_x\cos\phi_2 + \mathcal{P}_y\sin\phi_2$. The transverse polarizations of Ξ^- depend on phase differences which are defined by $\Delta_\pm = \zeta^-_{\pm\frac{1}{2}} - \zeta^+_{\pm\frac{1}{2}}$ and $\Delta^\pm = \zeta^\pm_{-\frac{1}{2}} - \zeta^\pm_{\frac{1}{2}}$ that lead to a relation $\Delta_+ - \Delta_- + \Delta^- - \Delta^+ = 0$. There are also other definitions of parity parameters for three-body system adopted in $\Lambda_c^+ \to pK^-\pi^+$ decay [37], and are relative to our parameters by

$$\begin{aligned} \mathcal{G}_0 &= \frac{\gamma^{\Xi_c^+} - 1}{\gamma^{\Xi_c^+} + 1}, \\ \mathcal{G}_1 &= \kappa_-\sin\Delta_- + \kappa_+\sin\Delta_+, \\ \mathcal{G}_2 &= \kappa_-\cos\Delta_- + \kappa_+\cos\Delta_+, \end{aligned} \tag{14}$$

where

$$\kappa_\pm = \frac{\sqrt{(1\pm\alpha_{\Xi_c^+})(1\pm\beta_{\Xi_c^+})\gamma_{\Xi_c^+}}}{1+\gamma_{\Xi_c^+}}. \tag{15}$$

When parity is conserved, the values of parameters $\mathcal{G}_1$ and $\mathcal{G}_2$ can not be determined directly due to their undetermined phases in Eq. (14), while $\alpha_{\Xi_c^+} = \beta_{\Xi_c^+} = 0$ that provides more freedoms for cross testing of parity violations.

C. Cascade decays and joint angular distributions

The dominate processes for Ξ^- decay are $\Xi^- \to \Lambda\pi^-$ and $\Lambda \to p\pi^-$. Their helicity angles and amplitudes are defined in Sec. II, and the asymmetry parameter of the spin-$\frac{1}{2}$ baryons for the decay $\Xi^- \to \Lambda\pi^-$ can be defined as

$$\alpha_{\Xi^-} = \frac{|F_{\frac{1}{2}}|^2 - |F_{-\frac{1}{2}}|^2}{|F_{\frac{1}{2}}|^2 + |F_{-\frac{1}{2}}|^2}. \tag{16}$$

The parameter α_Λ for $\Lambda \to p\pi^-$ has a similar expression. The latest measurements of the two parameters are $\alpha_{\Xi^-} = -0.367^{+0.005}_{-0.006}$ and $\alpha_\Lambda = 0.746 \pm 0.008$ from the Particle Data Group (PDG) [38]. Carrying out an equation analog to Eq. (11), the unpolarized and longitudinal parts of Λ can be obtained, they are

$$\mathcal{P}_0^\Lambda = \frac{2\mathcal{P}_0^{\Xi^-}}{1+\alpha_{\Xi^-}}\Big[1 + \alpha_{\Xi^-}\cos\theta_3\mathcal{P}_z^{\Xi^-} + \alpha_{\Xi^-}\sin\theta_3\left(\cos\phi_3\mathcal{P}_x^{\Xi^-} + \sin\phi_3\mathcal{P}_y^{\Xi^-}\right)\Big], \tag{17}$$

$$\mathcal{P}_0^\Lambda\mathcal{P}_z^\Lambda = \frac{2\mathcal{P}_0^{\Xi^-}}{1+\alpha_{\Xi^-}}\Big\{\alpha_{\Xi^-} + \cos\theta_3\mathcal{P}_z^{\Xi^-} + \sin\theta_3\left(\cos\phi_3\mathcal{P}_x^{\Xi^-} + \sin\phi_3\mathcal{P}_y^{\Xi^-}\right)\Big\}. \tag{18}$$

The SDM of proton can be obtained in a same way, and the angular distribution is given by $\mathcal{W} = \mathrm{Tr}\rho^p$, which is similar to Eq. (17) but in terms of polarizations of Λ. Next the distributions for polar angles can be obtained by integrating out other angles, and the nontrivial distributions are

$$\frac{dN}{d\phi_1} \propto 1 + \alpha_c\frac{1+2p_T^2}{3}\cos 2\phi_1, \tag{19}$$

$$\frac{dN}{d\cos\theta_1} \propto 1 + \alpha_c\cos^2\theta_1, \tag{20}$$

$$\frac{dN}{d\cos\theta_3} \propto 1 + \alpha_{\Xi^-}\frac{g_+^{\Xi^-}}{f_+^{\Xi^-}}\cos\theta_3, \tag{21}$$

$$\frac{dN}{d\cos\theta_4} \propto 1 + \alpha_{\Xi^-}\alpha_\Lambda\cos\theta_4, \tag{22}$$

where the distribution of $\cos\theta_1$ is free of beam polarization, and the last distribution Eq. (22) is known in Ref. [38] while the distribution of $\cos\theta_2$ is flat. The distribution of $\cos\theta_3$ is effected by parity parameters of Ξ_c^+ through $g_+^{\Xi^-}/f_+^{\Xi^-} = (\beta_{\Xi_c^+} + \alpha_{\Xi_c^+}\gamma_{\Xi_c^+})/(1+\gamma_{\Xi_c^+})$. The plots for Eq. (19) and Eq. (21) are given in Fig. 3 and Fig. 4 respectively. Under the assumption of parity conversation that $\alpha_{\Xi^-} = 0$ for $\Xi^- \to \Lambda\pi^-$ or $g_+^{\Xi^-} = 0$ for $\Xi_c^+(\lambda_1) \to \Xi^-(\lambda_2)\pi^+\pi^+$, the distributions turn to be constants respectively. Otherwise when parity violation exists, the absolute amplitudes of the distributions for $\cos\theta_3$ are non-zero.

The angular distribution after normalization is defined by

$$\widetilde{\mathcal{W}} = \frac{\mathcal{W}(\theta_i,\phi_i,\alpha_i)}{\int\Pi_i^4 d\cos\theta_i\phi_i\mathcal{W}(\theta_i,\phi_i,\alpha_i)}. \tag{23}$$

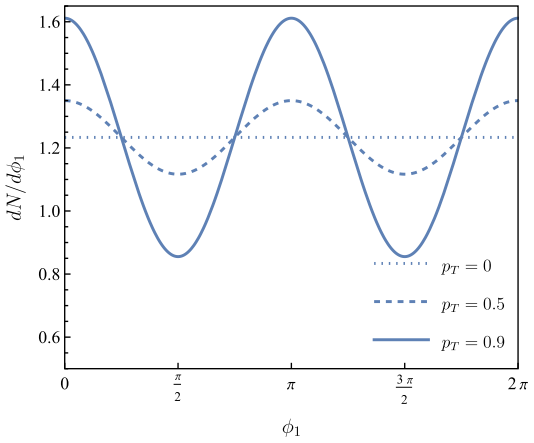

Fig. 3. (color online) Angular distributions of ϕ_1 for $p_T = 0$, 0.5, 0.9 (dotted, dashed and solid lines, respectively).

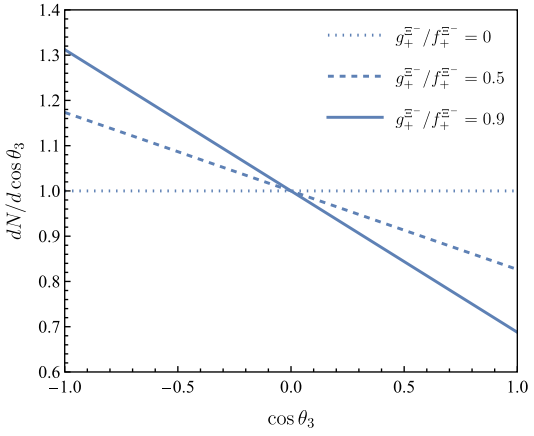

Fig. 4. (color online) Angular distributions of $\cos\theta_3$ for $g_+^{\Xi^-}/f_+^{\Xi^-} = 0$, 0.5, 0.9 (dotted, dashed and solid lines, respectively).

It is directive to define the weighted polarizations of Ξ_c^+ depending on θ_1 or ϕ_1 by integrating out other angles to get

$$\frac{d\langle\mathcal{P}_0\rangle}{d\cos\theta_1} \propto 1+2\alpha_c\cos^2\theta_1+\alpha_c^2\left(\cos^4\theta_1+\frac{p_T^4}{2}\sin^4\theta_1\right), \tag{24}$$

$$\frac{d\langle\mathcal{P}_0\rangle}{d\phi_1} \propto 1+\frac{2}{3}\alpha_c(1+2p_T^2\cos 2\phi_1) + \frac{\alpha_c^2}{5}\left(1+\frac{4}{3}p_T^2\cos 2\phi_1+\frac{8}{3}p_T^4\cos^2(2\phi_1)\right), \tag{25}$$

$$\frac{d\langle\mathcal{P}_y\rangle}{d\phi_1} \propto (1-p_T^2\cos 2\phi_1)\sin\phi_1, \tag{26}$$

$$\frac{d\langle\mathcal{P}_x\rangle}{d\phi_1} \propto p_T^2\sin 2\phi_1, \tag{27}$$

and $d\langle\mathcal{P}_z\rangle/d\phi_1 = 0$. The corresponding plots are shown in Fig. 5, 6, 7 and 8 respectively. The beam polarization enhances the polarizations distributions of ϕ_1, but suppress the unpolarization distribution of $\cos\theta_1$.

For the observed data sample of N events, the likelihood function is expressed as [39]

$$L(\theta_i,\phi_i,\alpha_c,\alpha_{\Xi^-},\alpha_\Lambda,\alpha_{\Xi_c^+},\beta_{\Xi_c^+},\gamma_{\Xi_c^+}) = \prod_{i=1}^{N}\widetilde{\mathcal{W}}_j, \tag{28}$$

where θ_i and ϕ_i represent polar angle and azimuth angle, and α_c, α_{Ξ^-}, α_Λ, $\alpha_{\Xi_c^+}$, $\beta_{\Xi_c^+}$, and $\gamma_{\Xi_c^+}$ mean decay parameters, and the product is computed based on the probability of the i-th event $\widetilde{\mathcal{W}}_j$. Here, α_{Ξ^-} and α_Λ are fixed to PDG values [38]. According to the maximum likelihood method, the relative uncertainty for estimating statistical sensitivity to parity parameter $\alpha_{\Xi_c^+}$ is defined as

$$\delta(\alpha_{\Xi_c^+}) = \frac{\sqrt{V(\alpha_{\Xi_c^+})}}{|\alpha_{\Xi_c^+}|}, \tag{29}$$

where the inverse of the variance is given by

$$V^{-1}(\alpha_{\Xi_c^+}) = N\int\frac{1}{\widetilde{\mathcal{W}}}\left[\frac{\partial\widetilde{\mathcal{W}}}{\partial\alpha_{\Xi_c^+}}\right]^2\prod_i^4 d\cos\theta_i d\phi_i. \tag{30}$$

Indeed for identifying significance of CP violations, the statistical sensitivity of $\mathcal{A}_{CP}$ in Eq. (4) can be estimated if $\alpha_{\Xi_c^+}$ and $\bar{\alpha}_{\Xi_c^-}$ are considered as non-correlation, via error propagation formula:

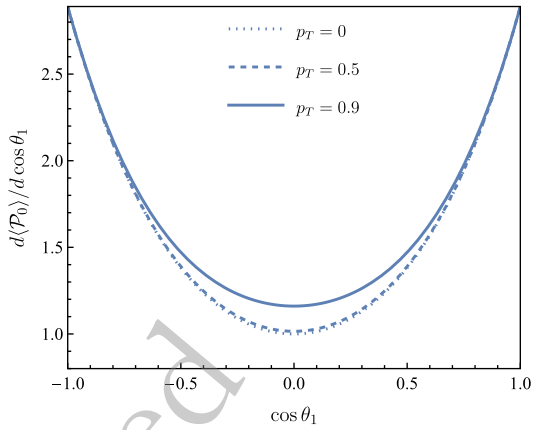

Fig. 5. (color online) Weighted $\mathcal{P}_0$ as a function of $\cos\theta_1$ for $p_T = 0$, 0.5, 0.9 (dotted, dashed and solid lines, respectively).

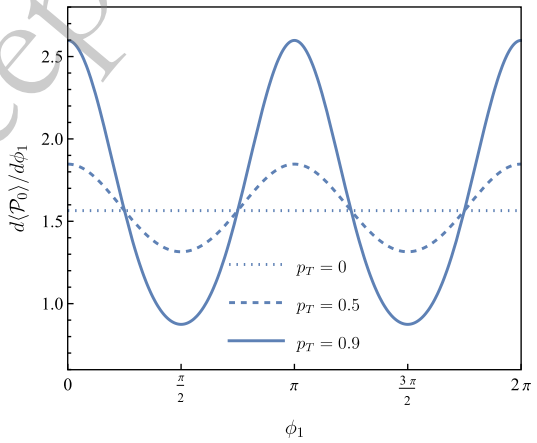

Fig. 6. (color online) Weighted $\mathcal{P}_0$ as a function of ϕ_1 for $p_T = 0$, 0.5, 0.9 (dotted, dashed and solid lines, respectively).

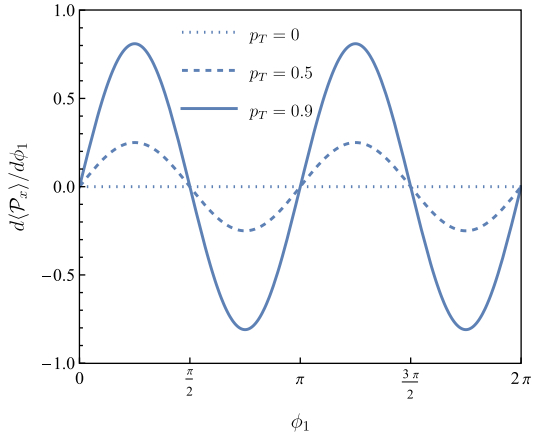

Fig. 7. (color online) Weighted $\mathcal{P}_x$ as a function of ϕ_1 for $p_T = 0$, 0.5, 0.9 (dotted, dashed and solid lines, respectively).

$$\delta(\mathcal{A}_{CP}) = \frac{2\sqrt{\alpha_{\Xi_c^+}^2\delta(\bar{\alpha}_{\bar{\Xi}_c^-})^2+\bar{\alpha}_{\bar{\Xi}_c^-}^2\delta(\alpha_{\Xi_c^+})^2}}{(\alpha_{\Xi_c^+}-\bar{\alpha}_{\bar{\Xi}_c^-})^2}, \tag{31}$$

where $\delta(\bar{\alpha}_{\bar{\Xi}_c^-})$ is the sensitivity for $\bar{\Xi}_c^-$ system. The sensit-

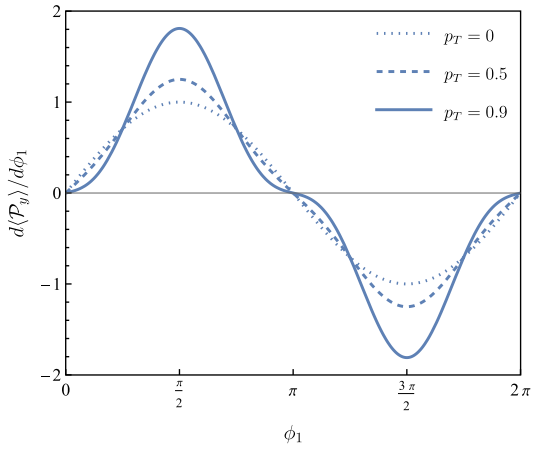

Fig. 8. (color online) Weighted $\mathcal{P}_y$ as a function of ϕ_1 for $p_T = 0,\ 0.5,\ 0.9$ (dotted, dashed and solid lines, respectively).

ivities $\delta(\mathcal{B}_{CP})$ and $\delta(C_{CP})$ for other two CP parameters can be defined in similar ways.

IV. NUMERICAL SENSITIVITIES

We are particularly interested in the dependence of statistical sensitivities on asymmetry parameters and beam polarizations. To clarify the analysis, we fix $\alpha_c = 0.7$, $\Delta_1 = \pi/6$, and $\Delta_\pm = \Delta^+ = \pi/3$. We have verified that other sets of phase angle values do not significantly affect the statistical quantities. In the following figures, when varying one parameter, the other two parameters are held constant. For example, the red lines in Fig. 9 illustrate the distributions of $\delta(\alpha_{\Xi_c^+})$ as functions of the event number N, with $\beta_{\Xi_c^+} = 0.1$ and $\gamma_{\Xi_c^+} = 0.5$ fixed. Similarly, the blue lines represent the distributions of $\delta(\beta_{\Xi_c^+})$ with $\alpha_{\Xi_c^+} = 0.1$ and $\gamma_{\Xi_c^+} = 0.5$, while the green lines show the distributions of $\delta(\gamma_{\Xi_c^+})$ with $\alpha_{\Xi_c^+} = 0.1$ and $\beta_{\Xi_c^+} = 0.3$. These sensitivities exhibit a negative correlation with the absolute values of the parameters. Under our chosen parameter values at $\alpha_{\Xi_c^+} = 0.5$ and $\beta_{\Xi_c^+} = 0.5$, the corresponding sensitivities reach 1% with about 3×10^3 signal events.

In Fig. 9, The statistical significance of $\gamma_{\Xi_c^+}$ is weak respected to $\alpha_{\Xi_c^+}$ and $\beta_{\Xi_c^+}$ under same signal events. However, $\delta(\gamma_{\Xi_c^+})$ has strong dependence on beam polarizations since its parameter is defined as the radio of two projections of angular momentum in Eq. (1). As exhibited in Fig. 10, the measurement accuracy of $\gamma_{\Xi_c^+}$ can be improved due to the beam polarization contribution. The significance of $\gamma_{\Xi_c^+}$ is also relative to intrinsic phases difference Δ_1 according to Eq. (10). If Δ_1 reach to saddle point $\pi/2$, the requirement of events decreases apparently and the corresponding curves are plotted in Fig. 11. In addition, we have test that $\alpha_{\Xi_c^+}$ and $\beta_{\Xi_c^+}$ sensitivities are not sensitive to p_T and Δ_1.

Next we consider the sensitivity estimation on CP violation parameter according to the error propagation

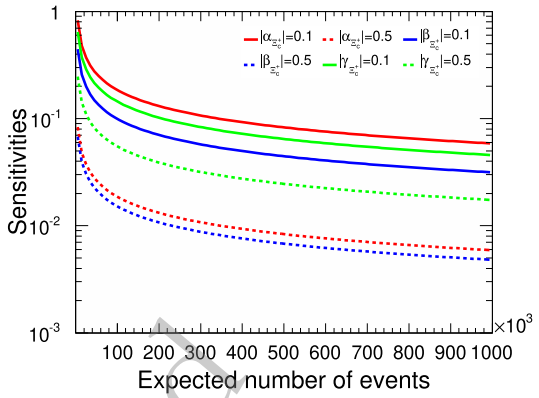

Fig. 9. (color online) The $\alpha_{\Xi_c^+}$, $\beta_{\Xi_c^+}$, and $\gamma_{\Xi_c^+}$ sensitivity distributions relative to signal yields in terms of different parameters. The red solid and dashed lines represent the $\alpha_{\Xi_c^+}$ values of 0.1 and 0.5, respectively. The blue solid and dashed lines represent the $\beta_{\Xi_c^+}$ values of 0.1 and 0.5, respectively. The green solid and dashed lines represent the $\gamma_{\Xi_c^+}$ values of 0.1 and 0.5, respectively.

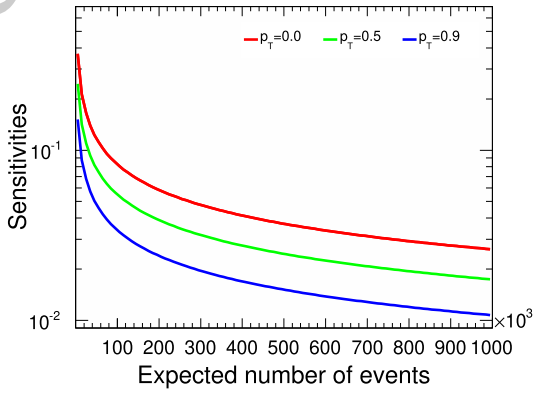

Fig. 10. (color online) The $\gamma_{\Xi_c^+}$ sensitivity distribution relative to signal yields assuming $\gamma_{\Xi_c^+} = 0.5$. The p_T values of 0.0, 0.5, and 0.9 correspond to the red, green, and blue lines, respectively.

equation Eq. (31). The CP violation in charm system should be more weak than that in bottom system [13], so we constraint the upper limit of the parameters like $\mathcal{A}_{CP} < 0.05$ and the plot for the sensitivity of this parameter is shown in Fig. 12 with using the bands to display uncertainty. The statistical significances for P and CP violations are positively correlated, but the latter one requires more events to reach same sensitivities. For example, we find the parity sensitivity is 0.01 when $N = 300000$, while CP sensitivity is about 0.04 by comparing lines in Fig. 9 and Fig. 12 for $\alpha_{\Xi_c^+} = 0.5$. The variations of $\mathcal{B}_{CP}$ and C_{CP} sensitivities on different parameters are shown in Fig. 13 and Fig. 14 respectively. In the last figure Fig. 15, we also show that the increasing of the polarization reduce the required events under the same significance for C_{CP} sensitivity.

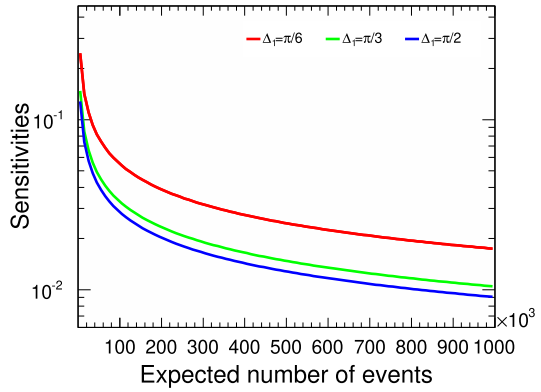

Fig. 11. (color online) The $\gamma_{\Xi_c^+}$ sensitivity distributions relative to signal yields assuming $\gamma_{\Xi_c^+}=0.5$. The Δ_1 values of $\pi/6$, $\pi/3$, and $\pi/2$ correspond to the red, green, and blue lines, respectively.

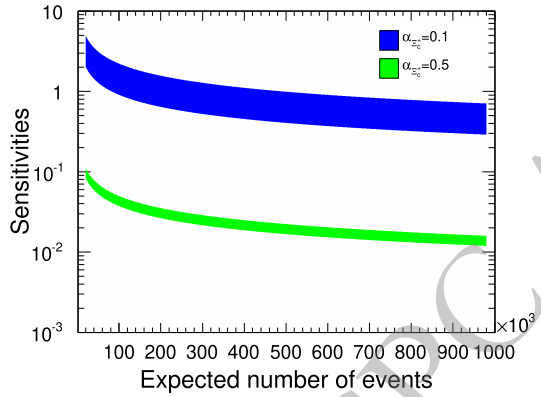

Fig. 12. (color online) The $\mathcal{A}_{CP}$ sensitivity distributions relative to signal yields. The $\alpha_{\Xi_c^+}$ values of 0.1 and 0.5 correspond to the blue and green bands, respectively.

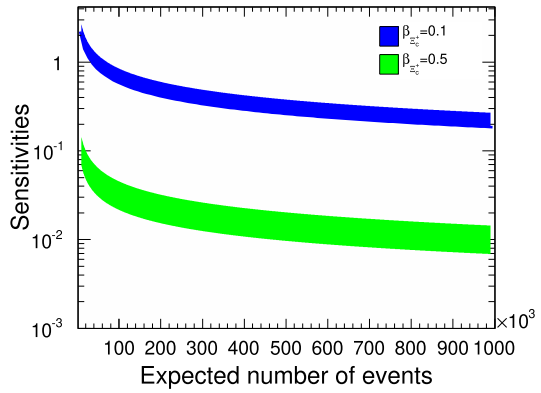

Fig. 3. (color online) The $\mathcal{B}_{CP}$ sensitivity distributions relative to signal yields. The $\beta_{\Xi_c^+}$ values of 0.1 and 0.5 correspond to the blue and green bands, respectively.

V. SUMMARY

The Cabibbo-favored three-body decay processes $\Xi_c^+\to\Xi^0\pi^+\pi^0$ and $\Xi_c^+\to\Xi^-\pi^+\pi^+$ represent the most probable decay modes of Ξ_c^+. The intermediate processes

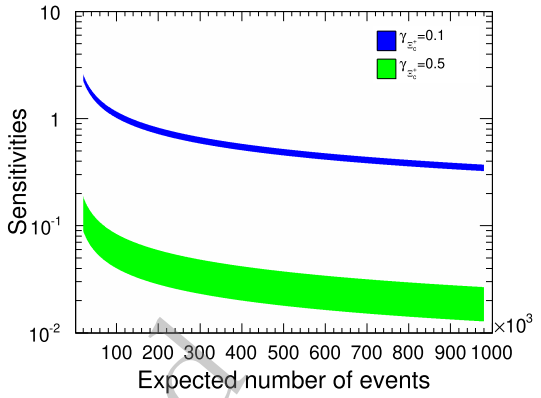

Fig. 14. (color online) The C_{CP} sensitivity distributions relative to signal yields. The $\gamma_{\Xi_c^+}$ values of 0.1 and 0.5 correspond to the blue and green bands, respectively.

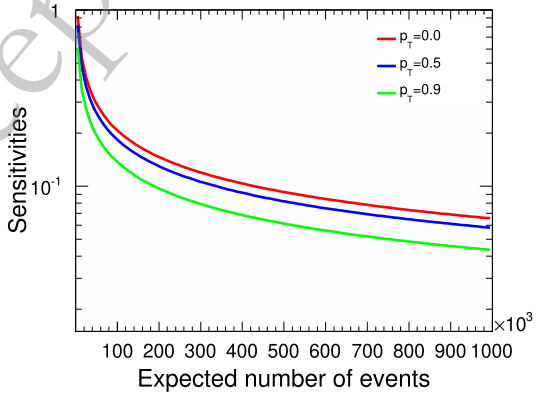

Fig. 15. (color online) The C_{CP} sensitivity distributions relative to signal yields assuming $\gamma_{\Xi_c^+}=0.5$. The red, blue, and green lines represent the p_T values of 0.0, 0.5, and 0.9, respectively.

$\Xi_c^+\to\Xi(1620)^0\pi^+\to\Xi^-\pi^+\pi^+$ and $\Xi_c^+\to\Xi(1690)^0\pi^+\to\Xi^-\pi^+\pi^+$ can also be measured with same method. By measuring the asymmetry decay parameters, the P and CP symmetries can be systematically tested. With sufficiently large data samples, the precision of the decay parameters $\alpha_{\Xi_c^+}$, $\beta_{\Xi_c^+}$, and $\gamma_{\Xi_c^+}$ can be significantly improved. Notably, for a given data sample, the measurement precision increases as the decay parameters approach 1. Experimentally, there are some challenges in achieving controllable beam polarization. However, the effect of beam polarization can significantly enhance the precisions of $\gamma_{\Xi_c^+}$ and $\mathcal{A}_{CP}$ measurements. Therefore, it is very important to achieve a controllable beam polarization in future experiments, especially in the precise study of CP. For instance, when the phase difference Δ_1 is close to $\pi/2$, and decay parameters are close to 1, the sensitivity becomes more obvious. The expected CP violation in $\Xi_c^+\to\Xi^-\pi^+\pi^+$ decay from weak interactions is on the order of 10^{-4} to 10^{-5}, which is suppressed respecting to a rough benchmark number 10^{-3} [40], and mesurement for $\mathcal{A}_{CP}$ and $\mathcal{B}_{CP}$ will provide a good constraint to

the total CP violation in this decay. Therefore, it is estimated that at least 1.0×10^9 $\Xi_c^+\bar{\Xi}_c^-$ events are required to observe CP violation, under the assumption of $\alpha_{\Xi_c^+}=0.5$. The process could serve as an excellent probe to search for new sources of CP violation beyond Standard Model. In this study, the sensitivities of the asymmetry parameters and CP for the decay $\Xi_c^+ \to \Xi^-\pi^+\pi^+$ are evaluated under various data sample sizes and beam polarization conditions. This work marks the first investigation of P and CP violation in the three-body decay of Ξ_c^+, providing essential theoretical support for future experiments, such as STCF.

References

[1] A. D. Sakharov, Pisma Zh. Eksp. Teor. Fiz. **5**, 32 (1967)
[2] N. Cabibbo, Phys. Rev. Lett. **10**, 531 (1963)
[3] M. Kobayashi and T. Maskawa, Prog. Theor. Phys. **49**, 652 (1973)
[4] J. H. Christenson, J. W. Cronin, V. L. Fitch and R. Turlay, Phys. Rev. Lett. **13**, 138 (1964)
[5] A. Abashian *et al.* (Belle Collaboration), Phys. Rev. Lett. **86**, 2509 (2001)
[6] B. Aubert *et al.* (BaBar Collaboration), Phys. Rev. Lett. **86**, 2515 (2001)
[7] Y. Chao *et al.* (Belle Collaboration), Phys. Rev. Lett. **93**, 191802 (2004)
[8] B. Aubert *et al.* (BaBar Collaboration), Phys. Rev. Lett. **93**, 131801 (2004)
[9] R. Aaij *et al.* (LHCb Collaboration), Phys. Rev. Lett. **122**, 211803 (2019)
[10] H. N. Li, C. D. Lü and F. S. Yu, arXiv: 1903.10638 [hep-ph].
[11] M. E. Peskin, Nature **419**, 24 (2002)
[12] R. Aaij *et al.* (LHCb Collaboration), Phys. Rev. Lett. **134**, 101802 (2025)
[13] R. Aaij *et al.* (LHCb Collaboration), Nature **643**, 1223 (2025)
[14] T. D. Lee, J. Steinberger, G. Feinberg, P. K. Kabir, and C. N. Yang, Phys. Rev. **106**, 1367 (1957)
[15] M. Ablikim *et al.* (BESIII Collaboration), Nature **606**, 64 (2022)
[16] M. Ablikim *et al.* (BESIII Collaboration), Phys. Rev. Lett. **129**, 131801 (2022)
[17] M. Ablikim *et al.* (BESIII Collaboration), Phys. Rev. Lett. **131**, 191802 (2023)
[18] M. Ablikim *et al.* (BESIII Collaboration), Phys. Rev. Lett. **125**, 052004 (2020)
[19] M. Ablikim *et al.* (BESIII Collaboration), [arXiv: 2503.17165 [hep-ex]].
[20] J. Tandean, Phys. Rev. D **69**, 076008 (2004)
[21] N. Salone, P. Adlarson, V. Batozskaya, A. Kupsc, S. Leupold and J. Tandean, Phys. Rev. D **105**, 116022 (2022)
[22] X. G. He, J. Tandean, and G. Valencia, Sci. Bull. **67**, 1840 (2022)
[23] X. G. He, H. Murayama, S. Pakvasa and G. Valencia, Phys. Rev. D **61**, 071701 (2000)
[24] E. Goudzovski, D. Redigolo, K. Tobioka, J. Zupan, G. Alonso-Álvarez, D. S. M. Alves, S. Bansal, M. Bauer, J. Brod and V. Chobanova, *et al.*, Rept. Prog. Phys. **86**, 016201 (2023)
[25] S. Navas *et al.* (Particle Data Group), Phys. Rev. D **110**, 030001 (2024)
[26] M. Achasov, X. C. Ai, R. Aliberti, L. P. An, Q. An, X. Z. Bai, Y. Bai, O. Bakina, A. Barnyakov and V. Blinov *et al.*, Front. Phys. (Beijing) **19**, 14701 (2024)
[27] T. D. Lee and C. N. Yang, Phys. Rev. **108**, 1645 (1957)
[28] S. U. Chung, (1971), 10.5170/CERN-1971-008.
[29] M. Mikhasenko *et al.* (JPAC), Phys. Rev. D **101**(3), 034033 (2020)
[30] J. P. Wang and F. S. Yu, Phys. Lett. B **849**, 138460 (2024)
[31] J. F. Donoghue, X. G. He and S. Pakvasa, Phys. Rev. D **34**, 833 (1986)
[32] M. Saur and F. S. Yu, Sci. Bull. **65**, 1428 (2020)
[33] M. G. Doncel, P. Mery, L. Michel, P. Minnaert and K. C. Wali, Phys. Rev. D **7**, 815 (1973)
[34] H. Chen and R. G. Ping, Phys. Rev. D **102**, 016021 (2020)
[35] X. Cao, Y. T. Liang, and R. G. Ping, Phys. Rev. D **110**, 014035 (2024)
[36] M. Ablikim *et al.* (BESIII Collaboration), Phys. Lett. B **770**, 217 (2017)
[37] D. H. Wei, Y. X. Yang and R. G. Ping, Chin. Phys. C **46**(7), 074002 (2022)
[38] S. Navas *et al.* (Particle Data Group), Phys. Rev. D **110**, 030001 (2024)
[39] T. Z. Han, R. G. Ping, T. Luo, and G. Z. Xu, Chin. Phys. C **44**, 013002 (2020)
[40] S. Bianco, F. L. Fabbri, D. Benson and I. Bigi, Riv. Nuovo Cim. **26**(7-8), 1 (2003)